Palaeogeography, Palaeoclimatology, Palaeoecology 268 (2008) 39–46

Contents lists available at ScienceDirect

Palaeogeography, Palaeoclimatology, Palaeoecology

journal homepage: www.elsevier.com/locate/palaeo

Vegetation and soil feedbacks at the Last Glacial Maximum

Dabang Jiang *

Nansen-Zhu International Research Centre, Institute of Atmospheric Physics, Chinese Academy of Sciences, Beijing, China
Max Planck Institute for Biogeochemistry, Jena, Germany

ARTICLE INFO

Article history:
Received 28 January 2008
Received in revised form 30 July 2008
Accepted 31 July 2008

Keywords:
Last Glacial Maximum
Vegetation feedback
Soil feedback
Simulation
Coupled model

ABSTRACT

Vegetation feedback at the Last Glacial Maximum (LGM, about 21,000 calendar years ago) remains an unresolved question. A global atmospheric general circulation model (AGCM) is asynchronously coupled with an equilibrium terrestrial biosphere model in the present study. The coupled model is then used to investigate the influences of vegetation and soil feedbacks on the LGM climate. It is found that the simulated geographical distribution of vegetation at the LGM differs from the present pattern dramatically, and glacial vegetation cover tends to be reduced on average. Vegetation feedback alone leads to an annual surface temperature decrease of 0.31 °C over the LGM ice-free continental areas. Additional soil feedback reinforced vegetation-induced cooling over high latitude Eurasia and from the eastern Middle East eastward to the Indian Peninsula significantly. In the tropics, a terrestrial annual surface cooling of 0.45 °C is produced by vegetation and soil feedbacks. It is shown that vegetation and soil feedbacks partly reduce data-model discrepancy as produced by the AGCM alone in some regions such as Central Africa, the Indian Peninsula, South China, and North Australia.

1. Introduction

A variety of climate states have been recorded in the Earth's history, and it is valuable to use climate models to simulate past climate intervals with significantly different climate conditions from the present. Such investigations can examine a model's sensitivity to varying external forcing conditions, and the lessons learned will improve our knowledge on the operation of climate regimes, which is undoubtedly helpful to understand current and future climate and climate change.

The LGM is a climate interval when the global climate differed greatly from the present, with more extensive ice sheets and sea ice, colder sea surface temperature (SST), and lower atmospheric CO_2 concentration. A series of proxy estimates and modelling exercises for the LGM climate have been performed in recent decades, especially within the framework of the Paleoclimate Modelling Intercomparison Project (PMIP) (Joussaume and Taylor, 1995). Many aspects of the reconstructed LGM climate have hitherto been reasonably well simulated, such as well-known global cooling, etc. (e.g., PMIP, 2000; Cane et al., 2006; Braconnot et al., 2007; Jansen et al., 2007). However, quantitative discrepancies between proxy estimates and model simulations still exist, largely on a regional scale. For instance, the models systematically underestimate winter cooling over Europe and the Mediterranean region as suggested from pollen-based data (e.g., Kageyama et al., 2006; Ramstein et al., 2007), the simulations with prescribed SST underestimate terrestrial cooling reconstructed from vegetation and speleothem records in the tropics excluding equatorial Africa, and the LGM aridity based on lake-level and pollen data is strongly underestimated by the models using computed SST within phase one of the PMIP (e.g., Pinot et al., 1999). The data-model disagreements reflect joint inadequacies in the formation of the model, in the specification of prescribed boundary conditions, in the design of numerical experiments, or in the coverage and interpretation of the paleoenvironmental data (e.g., Kutzbach et al., 1998). Considerable effort has been devoted to the above issues by various groups throughout the world.

As well known, vegetation is intrinsically an interactive component in the climate system. Different from the typical integration with the modern vegetation, several sensitivity experiments either with global or regional vegetation reconstructions have indicated that vegetation can play an important role in modifying terrestrial surface temperature response to the typical LGM forcings (Crowley and Baum, 1997; Wyputta and McAvaney, 2001; Jiang et al., 2003), although these simulations do not include interactive feedbacks between the atmosphere and vegetation. Coupled climate-vegetation models have been used to investigate vegetation feedback at the LGM as well, and the corresponding results indicated that vegetation feedback can partly reduce data-model discrepancies produced by climate models alone in some regions such as western Siberia (Kubatzki and Claussen, 1998; Levis et al., 1999; Crucifix and Hewitt, 2005; Jahn et al., 2005). Vegetation feedback has been regarded as an important potential process contributing to the LGM climate (Harrison and Prentice, 2003; Crucifix et al., 2005; Jansen et al., 2007). However, climatic responses due to vegetation feedbacks vary greatly, both in magnitude and sign, when we compare available simulations resulting from different

* Max Planck Institute for Biogeochemistry, Jena, Germany.
E-mail address: jiangdb@mail.iap.ac.cn.

0031-0182/$ – see front matter © 2008 Elsevier B.V. All rights reserved.
doi:10.1016/j.palaeo.2008.07.023

model systems (see Concluding remarks section for detail). A central theme in paleoclimate modelling is the investigation of different models' responses to the same or similar forcing conditions (Joussaume and Taylor, 1995), and the differences or similarities of these responses. Therefore, it is interesting to examine to what extent vegetation feedback influences the LGM climate in a new atmosphere–vegetation model system.

Soil is interactively associated with vegetation and climate on a varying time-scale. Climate and vegetation changes will inevitably give rise to soil change if the time-scale is long enough to allow soil to evolve. Therefore, it is relevant to alter soil characteristics together with changed vegetation for climates of the distant past. Prior studies have indicated that soil feedback can play an important role in African climate in the mid-Holocene (Kutzbach et al., 1996; Levis et al., 2004). However, soil is typically kept constant in the LGM climate simulations even if reconstructed climate and vegetation conditions differ from the present day. This begs the question what the impact of soil feedback on the LGM climate might be. In an attempt to address the above issues, an atmospheric general circulation model is asynchronously coupled with an equilibrium terrestrial biosphere model in the present study. The coupled system is then used to evaluate influences of vegetation feedback and vegetation-dominated change in soil characteristics on the LGM climate.

2. Model and experiment

The global atmospheric general circulation model used here was developed at the Institute of Atmospheric Physics, Chinese Academy of Sciences (IAP-AGCM). The IAP-AGCM solves dynamic and thermodynamic equations and the continuity equations for mass and water vapour. It has a horizontal grid resolution of 4° in latitude by 5° in longitude and 9 levels in the vertical with the top at 10 hPa. A brief description on the model was presented in Jiang et al. (2003), and more detail can be found in the references therein. To date, a number of simulations have been performed with the model, and a reasonable representation of many aspects of the modern climate has been obtained (e.g., Liang, 1996). In particular, the IAP-AGCM has been utilized to simulate paleoclimate at the mid-Holocene (e.g., Wang, 2002; Wei and Wang, 2004; Jin et al., 2006) and LGM (e.g., Jiang et al., 2003; Ju et al., 2007) as well as mid-Pliocene (e.g., Jiang et al., 2005), and to investigate East Asian climate transition during the Cenozoic era (e.g., Zhang et al., 2007a,b).

The equilibrium terrestrial biosphere model BIOME3 (Haxeltine and Prentice, 1996) is applied here. This model relies on ecophysiological constraints, resource availability, and competition among plant functional types to simulate potential natural vegetation. It has a horizontal grid resolution of 0.5° by 0.5°. The model inputs include atmospheric CO_2 concentration, latitude, soil texture, monthly surface temperature, precipitation, and total cloud amount. The model outputs involve 18 kinds of biomes. The BIOME3 is suitable for predicting responses of vegetation to climate change alone and both climate and atmospheric CO_2 concentration changes and has been proved to be able to reproduce the broad-scale patterns in potential natural vegetation for the current climate, excluding Antarctica (Haxeltine and Prentice, 1996). Moreover, the BIOME model series have also been widely used to simulate past vegetation changes, such as at the mid-Holocene (e.g., Texier et al., 1997; Prentice et al., 1998; Kaplan et al., 2003) and the LGM (e.g., Jolly and Haxeltine, 1997; Kaplan et al., 2003).

As a first step, the horizontal resolution of the original observational climate data package used to drive BIOME3 (Leemans and Cramer, 1991) is converted into the grid mesh of the IAP-AGCM under the modern conditions using an area-averaged extrapolation approach. Therein, an atmospheric temperature lapse rate of 0.65 °C per 100 m is assumed when dealing with topography-induced surface temperature difference among the grids. The BIOME3 is then adjusted to be suitable for the LGM land–sea distribution (Peltier, 2004) by adding more land grid boxes, due to sea level lowering at the LGM, applying a climate data package based on that of the nearest-neighbour grid box at the same latitude. The broad agreement of the modern potential natural biome patterns over the LGM ice-free continents between the two panels as displayed in Fig. 1 demonstrates that the conversion of the BIOME3 horizontal resolution is reliable. In addition, the Earth's orbital parameters and atmospheric CO_2 concentration in BIOME3 are modified to the LGM configuration (see next paragraph). Since the biomes simulated by BIOME3 need to be used to drive the IAP-AGCM, the 18 kinds of biomes in the former are translated into the observation-based 10 categories in the latter, derived from the observation data with 1°×1° resolution and 32 classifications (Matthews, 1983), according to biome definition. In this

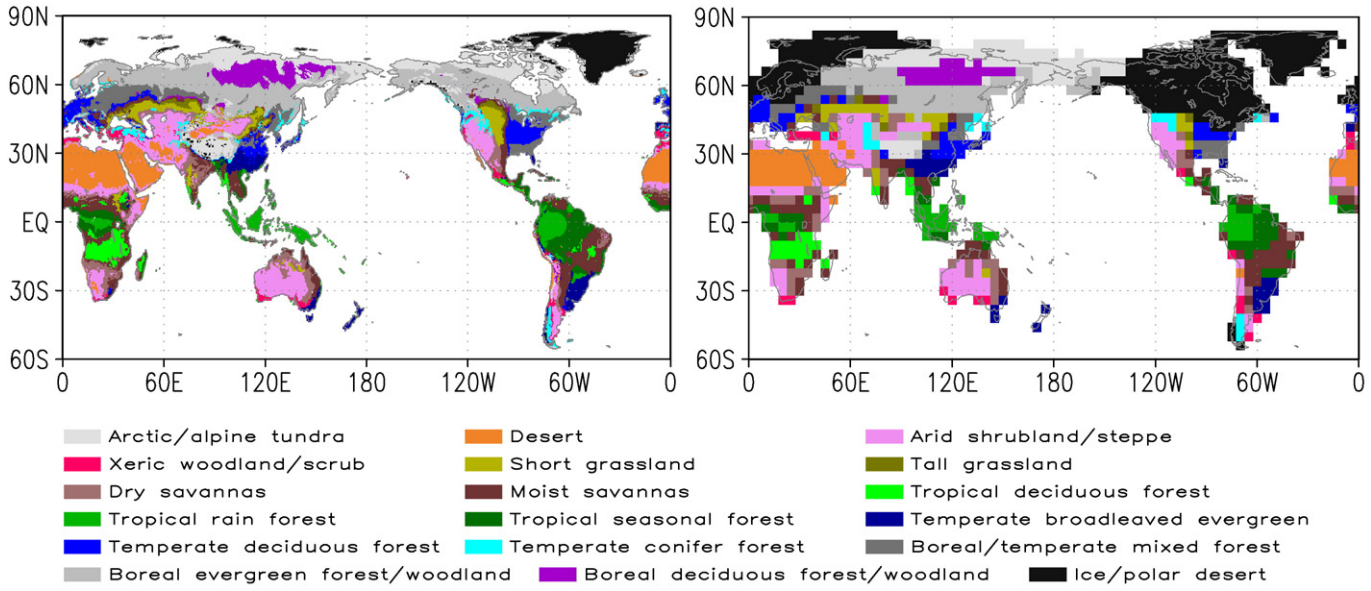

Fig. 1. The geographical distribution of the modern potential natural vegetation as simulated by BIOME3: the left panel is derived from the original BIOME3 with 0.5°×0.5° resolution, and the right panel is derived from the adjusted BIOME3 with 5°×4° resolution under the LGM land–sea distribution and continental ice sheet (Peltier, 2004).

way, the IAP-AGCM is interactively and asynchronously coupled with BIOME3.

Four numerical experiments have been performed, hereinafter referred to as RC, RL, RLV, and RLVS. The RC is the control run for the present climate, and atmospheric CO_2 concentration is held at 345 ppmv in line with the protocol of the PMIP. The RL is designed as a standard PMIP simulation for the LGM climate with the modern vegetation. The conditions that are adjusted to the LGM configuration are the Earth's orbital parameters (Berger, 1978), an atmospheric CO_2 concentration of 200 ppmv (e.g., Barnola et al., 1987), the continental ice sheet, topography and coastline (Peltier, 2004), and SST and sea ice (CLIMAP project members, 1981). Taking into account that there are differences between the present topography (Peltier, 2004) or SST (CLIMAP project members, 1981) data and those used in the IAP-AGCM control run, the final topography and SST data utilized in the RL are respectively obtained by keeping their values in the RC and adding to each of the two variables the differences between the LGM and the present as respectively calculated from Peltier (2004) and CLIMAP project members (1981). It should be noted that the above approach is different from that of Jiang et al. (2003), who took the reconstructed topography (Peltier, 1994) and SST (CLIMAP project members, 1981) values for the LGM directly. In the RC and RL, the IAP-AGCM is consecutively integrated for 30 years with the observation-based modern vegetation (Matthews, 1983), and the results analyzed below are averaged for the final 24 years, allowing the first 6 years for the model to reach a relative equilibrium state (Supplementary Material Figure S.1).

The RLV is performed by the coupled IAP-AGCM/BIOME3 system. Firstly, the monthly climatology of the last 24 years in the RC is chosen as the baseline. The monthly climatology difference between the last 5 years in the RL and the baseline is then added to the original climatology in BIOME3, and the vegetation stemming from the climate difference between the RL and the RC is consequently generated. Based on the earlier experiments (Claussen, 1994, 1997; Kubatzki and Claussen, 1998), the IAP-AGCM, additionally forced by the above vegetation scenario, relative to the RL, is integrated for 6 years for the first iteration in the RLV. The first year is taken as adjustment time. The monthly climatology difference between the remaining five years and the baseline is then superposed on the original climatology in BIOME3 again so as to generate a new vegetation scenario for next iteration. Seven iterations are performed in the RLV. Different from the first six iterations, the seventh iteration is integrated for 20 years in order to attain enough samples, i.e. the last 19 years' outputs being analyzed below, for evaluation of statistical significance by the use of a student *t*-test. It should be noted that the percentage difference of monthly precipitation with respect to the baseline is calculated and then added to the original climatology in BIOME3 in each of the iterations in order to reduce the influence of systematic model biases, taking into account precipitation divergences between the baseline simulation in the RC and the original observational climatology used to drive BIOME3. Unlike surface temperature and precipitation, monthly total cloud amount is held constant throughout because large uncertainties still remain when state-of-the-art climate models are used to reproduce total cloud amount.

Based on the RLV, it is additionally assumed in the RLVS that if newly simulated vegetation differs from that of the last iteration at any one grid box, the corresponding soil characteristics are then modified to match those at a proximal grid box that is covered with the newly simulated vegetation. In the IAP-AGCM, soil characteristics are prescribed as surface boundary conditions and include soil colour and texture, both of which are constructed from the Wilson and Henderson-Sellers (1985) data. The former is comprised of eight classes varying from light to dark, and the latter is comprised of eleven types, i.e. sand, loamy sand, sandy loam, silt loam, loam, sandy clay loam, silt clay loam, clay loam, sandy clay, silt clay, and light clay. Soil characteristics are intrinsically involved in the land surface processes and land–atmosphere interaction in the IAP-AGCM, particularly for surface albedo (for more detail, see Liang, 1996). Other aspects in the RLVS are consistent with the RLV. On the whole, the coupled IAP-AGCM/BIOME3 system runs stably in the RLV and RLVS, especially after the first four iterations. Moreover, the global surface temperature value in the first year is not largely different from that in the other years in each of the seven iterations (Supplementary Material Figure S.2). That means that one year is enough for the IAP-AGCM to adjust, consistent with the conclusion previously drawn by Claussen (1994, 1997).

3. Results

3.1. The LGM climate

At the LGM, climate conditions as simulated by the IAP-AGCM alone differ from the present greatly. The annual surface temperature is significantly lowered on a global scale (left panel in Fig. 2). On the whole, surface cooling amplifies towards high latitudes and is characterized by a larger magnitude over the continents than over the ocean. A global annual-average surface temperature decrease of 5.68 °C is obtained, comparable with the reconstructed value of about 5 °C (Cane et al., 2006; Jansen et al., 2007). Terrestrial annual surface temperature is reduced on average by 6.70 °C. In the tropics (30 °S–30 °N), terrestrial annual surface temperature cools on average by 2.08 °C, with a much larger amplitude in the northern tropics. By

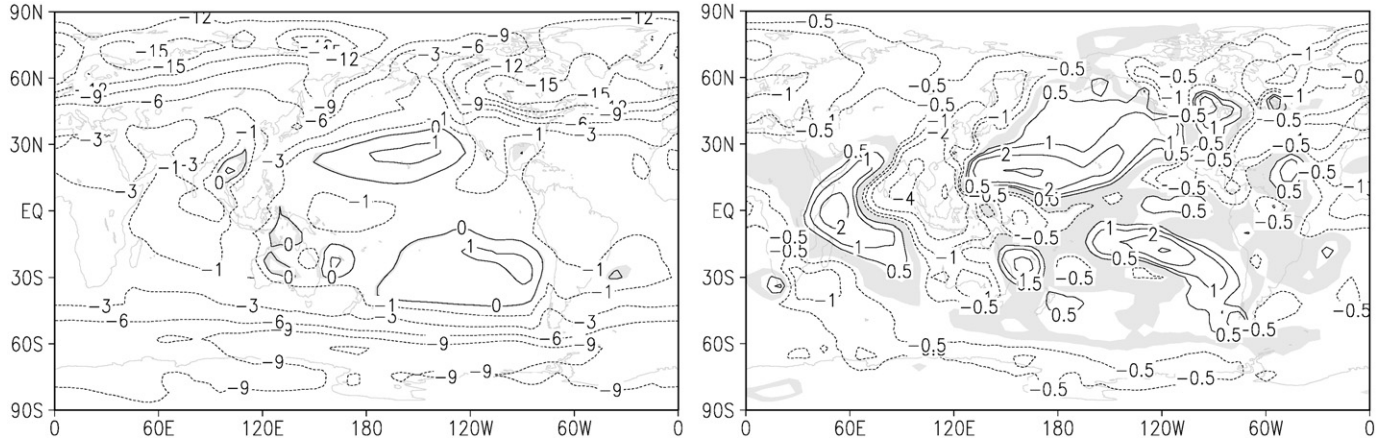

Fig. 2. The differences of mean annual surface temperature (left, unit: °C) and precipitation (right, unit: mm/day) between the LGM and the present (RL minus RC) as simulated by the IAP-AGCM alone. The areas with confidence level below 95% are shaded.

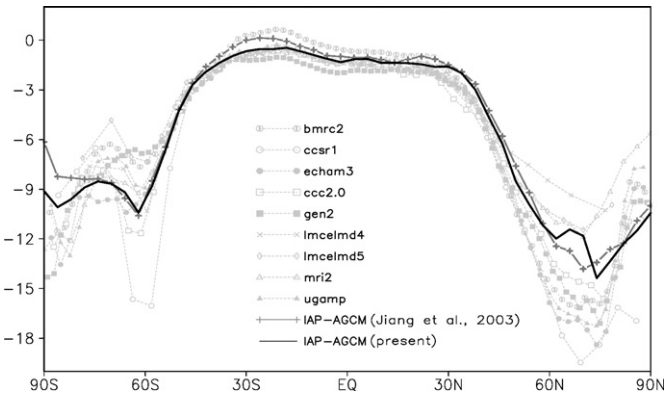

Fig. 3. Zonally-averaged differences of mean annual surface temperature between the LGM and the present as simulated by the PMIP fixed-SST AGCMs and the IAP-AGCM (unit: °C).

contrast, annual surface temperature warms somewhat over much of the mid-latitude Pacific Ocean in both hemispheres where warmer-than-today SST was compiled by CLIMAP project members (1981).

Climate is drier at the LGM as a whole, especially over continents (right panel in Fig. 2). Globally averaged annual precipitation is lowered by 10.3%, and terrestrial annual precipitation is lowered by 25.2%. The percentage change of annual precipitation is larger towards high latitudes, with decreases of 52.9%, 13.3%, 3.6%, −1.3%, 4.3%, and 30.8% within the 60°–90°N, 30°–60°N, 0°–30°N, 0°–30°S, 30°–60°S, and 60°–90°S latitude bands, respectively. The precipitation reduction is particularly noteworthy in East and South Asia with an average value of above 1 mm/day, which can be mostly ascribed to a significantly weakened summer monsoon system. By contrast, annual precipitation is enhanced over most parts of the Pacific Ocean, owing to the reconstructed warmer-than-today SST pattern (CLIMAP project members, 1981).

Compared to the prior simulation with the IAP-AGCM (Jiang et al., 2003), new reconstruction data of global ice sheet and topography, i.e. ICE-5G (Peltier, 2004), are used in the RL, in lieu of the prior ICE-4G (Peltier, 1994). In addition, the approach used to obtain the LGM SST and topography is also different (paragraph 4 in Section 2). The simulated LGM climate here is therefore somewhat different from the previous one, such as having a stronger surface cooling over central North America and much of northwestern Europe but a weaker surface cooling within 120°E-120°W and 60°–70°N. However, the geographical distribution of differences both in mean annual surface temperature and precipitation between the LGM and the present as simulated here is broadly consistent with Jiang et al. (2003), although there are discrepancies on a regional scale (figures omitted). Additionally, it can be seen in Fig. 3 that the IAP-AGCM results are overall in accordance with the simulations performed by the PMIP AGCMs with prescribed SST.

3.2. Vegetation and soil feedbacks

The coupled IAP-AGCM/BIOME3 system generates a dramatically different glacial vegetation distribution from the present pattern. Over the LGM ice-free continental areas, roughly 70% of the simulated

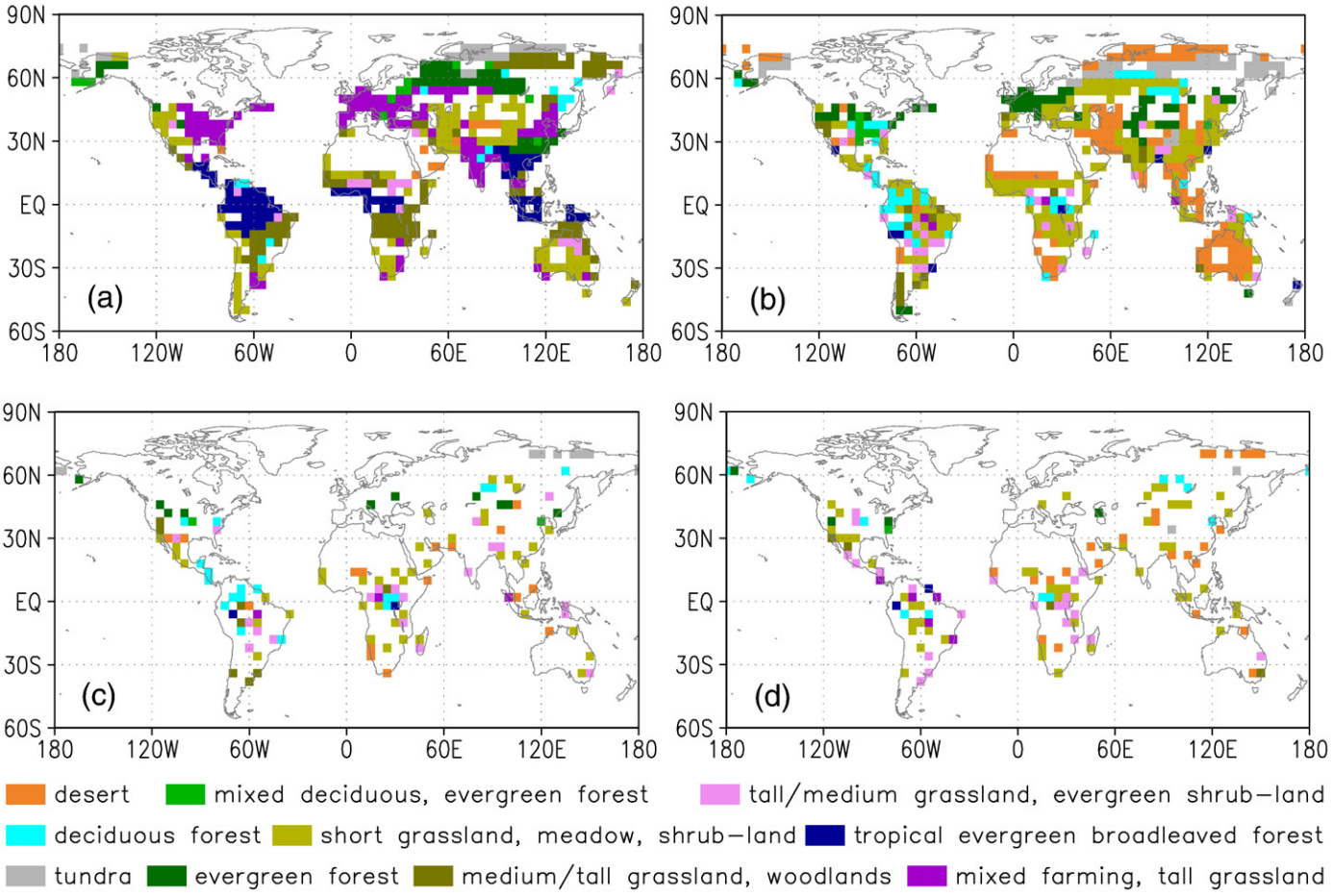

Fig. 4. The differences of vegetation over the LGM ice-free continental areas between the RL (a, i.e. the observed modern vegetation prescribed in the RL) and the RLV (b, i.e. the LGM vegetation simulated by the IAP-AGCM/BIOME3 in the RLV), and the differences between the RLV (c) and RLVS (d). In panels a and b (c and d), the continental areas covered with the same vegetation between the RL and RLV (RLV and RLVS) are in white.

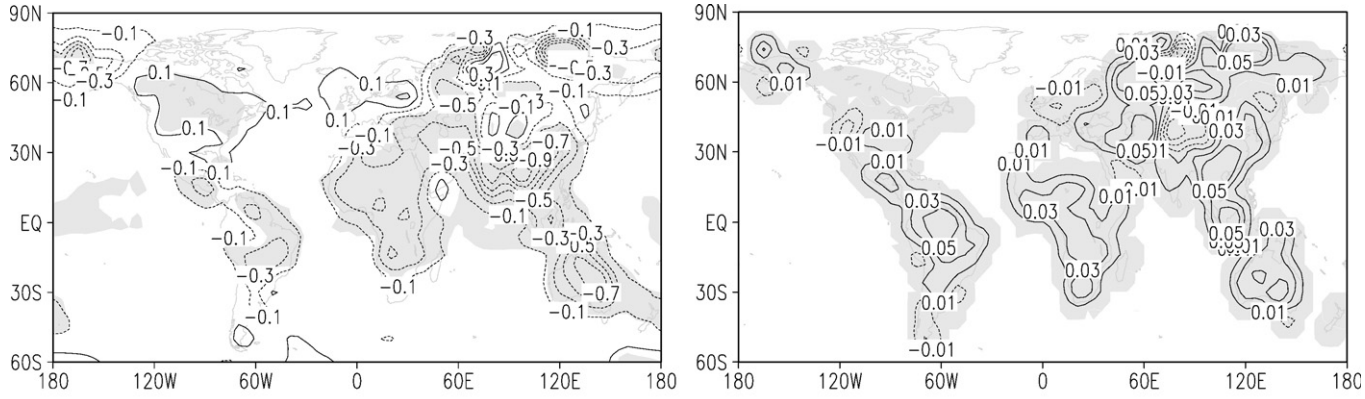

Fig. 5. The simulated differences of mean annual surface temperature (left, unit: °C) and albedo (right) between the RLV and the RL. The areas with confidence level above 95% are shaded.

vegetation in the RLV last iteration differs from that in the RL (upper row panels in Fig. 4). Relative to the RL, of most significance is that desert occupies northernmost Eurasia, Australia, eastern Middle East, and Southeast Asia in the RLV. Moreover, tundra appears at the expense of the present grassland and shrub in parts of northern Eurasia. The present tropical evergreen broadleaved forest is degraded into other biomes in much of tropical America within 10°S–20°N and in part of tropical Africa and Southeast Asia. Vegetation substitution is also registered in most parts of southern Africa, southern North America, and the Eurasian interior. A preliminary data-model comparison indicates that the sparser-than-today LGM vegetation cover as simulated here agrees qualitatively with proxy estimates on a large scale (Crowley, 1995; Adams and Faure, 1997; Prentice et al., 2000; Bigelow et al., 2003), although the nature of the LGM vegetation has been a matter of debate.

According to the experiments RLV and RL, the influence of vegetation feedback on global surface temperature is weak. It only induces an additional surface cooling of 0.07 °C on a global scale. However, vegetation feedback has a statistically significant impact on the annual surface temperature over much of the ice-free continents at the LGM (left panel in Fig. 5). Annual surface temperature is further reduced on average by 0.32 °C, 0.19 °C, 0.43 °C, 0.35 °C, and 0.09 °C over the LGM ice-free continental areas within the 60°–90°N, 30°–60°N, 0°–30°N, 0°–30°S, and 30°–60°S latitude bands, respectively. Surface cooling is more vigorous over northern Eurasia, Australia, and tropical continental areas excluding southern North America. It is found that the above cooling can be mostly attributed to vegetation-induced surface albedo change. As already mentioned above, the simulated vegetation in the RLV is generally sparser than that in the RL. The resultant surface albedo is larger (right panel in Fig. 5). For this reason, more solar short-wave radiation is reflected back into the sky in the RLV, leading to a lower surface temperature.

The RLVS reveals that soil feedback can induce additional vegetation and climate changes at the LGM. Roughly 18% of the LGM ice-free continental areas are covered with different biomes in the RLVS with respect to the RLV (lower row panels in Fig. 4). The changes occur mainly in South America, southern North America, tropical Africa within 10°S–10°N, eastern Eurasian interior, and northeastern-most Eurasia. In general, vegetation cover becomes somewhat sparser in the RLVS, although no systematic substitution emerges compared to the RLV. Concomitantly, roughly 47% (48%) of the LGM ice-free continental areas are given different values of soil colours (textures) in the RLVS with respect to the RLV (figures omitted).

Relative to the RLV, soil feedback further induces a globally averaged annual surface cooling of 0.05 °C, comparable with the value attained by vegetation feedback. Statistically significant surface cooling is mainly registered in northern Eurasia north of about 60°N, with a mean value of below −0.5 °C, and from around the eastern Middle East to the Indian Peninsula (left panel in Fig. 6). Annual surface temperature is reduced on average by 0.42 °C and 0.11 °C over the LGM ice-free continental areas within the 60°–90°N and 0°–30°N latitude bands in the RLVS compared with the RLV. The zonally-averaged difference of mean annual surface temperature between the RLVS and the RLV indicates that soil feedback further reinforces vegetation-induced cooling within the 58°–82°N and 14°–30°N latitude bands notably, although its global impact remains limited. It is found that the statistically significant cooling due to soil feedback can be mostly attributed to larger surface albedo in the RLVS than that

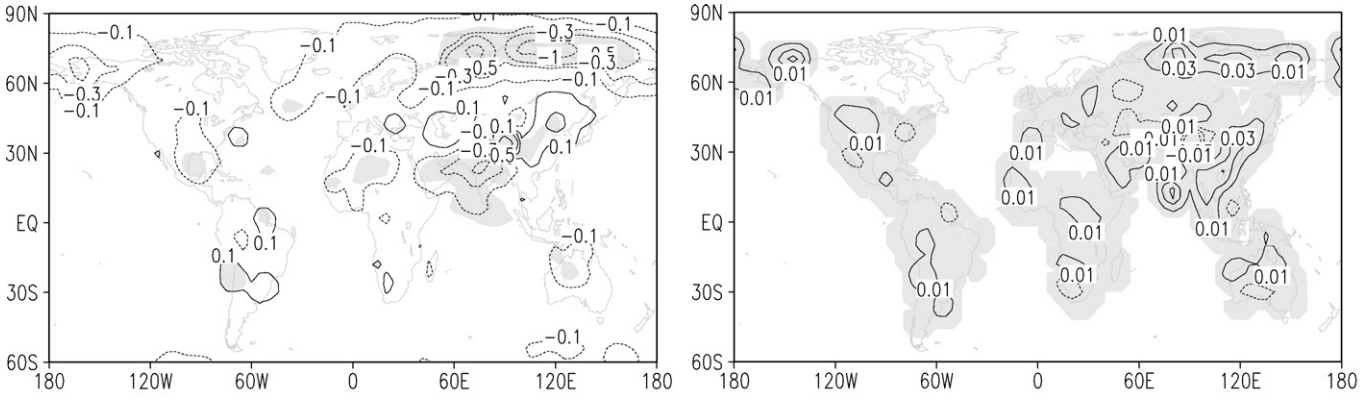

Fig. 6. The simulated differences of mean annual surface temperature (left, unit: °C) and albedo (right) between the RLVS and the RLV. The areas with confidence level above 95% are shaded.

Table 1
Data-model comparison for surface temperature (Unit: °C)[a]

Regions	Proxy estimates (LGM minus the present)			IAP-AGCM and/or coupled IAP-AGCM/BIOME3						
	MAT	MTCO	Error	MAT			Std			
				RL minus RC	RLV minus RL	RLVS minus RLV	RC	RL	RLV	RLVS
A	−5		20–50%	−1.28	0.02	−0.06	0.38	0.31	0.27	0.29
B		−3 to −6	20–50%	−1.63	−0.19	0.07	0.29	0.28	0.30	0.26
C	−7 to −6		20–50%	−3.23	−0.42	−0.04	0.34	0.27	0.30	0.27
D	−5.5		20–50%	−1.76	−0.16	0.09	0.32	0.31	0.28	0.27
E		−3 to −5	20–50%	−2.31	−0.38	−0.02	0.26	0.22	0.21	0.20
F	−12 to −8			−10.95	−0.11	−0.19	0.58	0.68	0.54	0.51
G	−6 to −5		20–50%	−2.41	−0.74	−0.32	0.33	0.43	0.39	0.36
H	−5 to −10			−1.99	−0.42	0.15	0.35	0.32	0.34	0.31
I	−7		±3.5	−0.97	−0.77	0.07	0.36	0.37	0.35	0.29
J	−3		±2	−1.14	−0.54	−0.12	0.35	0.30	0.25	0.27

[a] MAT denotes mean annual surface temperature, MTCO denotes mean surface temperature of the coldest month, and Std denotes standard deviation of MAT in each of the four experiments. Regions A: Western North America (95°–115°W, 30°–38°N), B: Northern South America (50°–75°W, 10°N–2°S), C: Central Africa (5°–15°E, 10°–18°N), D: South Africa (15°–35°E, 18°–30°S), E: Equatorial eastern Africa (25°–40°E, 2°N–10°S), F: North Russia (60°–75°E, 54°–66°N), G: India (75°–85°E, 10°–30°N), H: Middle-eastern China (100°–120°E, 30°–42°N), I: South China (105°–120°E, 22°–30°N), and J: North Australia (135°–150°E, 14°–22°S). For proxy estimations, see Farrera et al. (1999) for regions A, B, C, D, E, G, I, and J, Tarasov et al. (1999) for F, and Yu et al. (2001) for H.

in the RLV (right panel in Fig. 6), which results from changes in vegetation and/or soil characteristics. With respect to the RLV, for instance, the soil colour becomes lighter and desert takes the place of tundra in northern Eurasia, and soil colour becomes lighter and soil texture changes notably in the eastern Middle East to the Indian Peninsula in the RLVS.

On the whole, the influence of vegetation feedback on precipitation is weak. A statistically significant annual precipitation decrease of 0.1–0.5 mm/day occurs in much of tropical Africa within 30°S–15°N, Southeast Asia, and northern South America. On the contrary, annual precipitation increases by 0.1–0.8 mm/day in the central and western tropical North Pacific Ocean, which mostly arises from the June–July–August (JJA) precipitation increase. During JJA, vegetation feedback induces additional cooling over the East and South Asian continental areas, and the thermal contrast between the Asian continent and the Pacific Ocean is hence decreased. As a result, the subtropical high over the western North Pacific Ocean is weakened. Meanwhile, an anomalous easterly belt originates from northern South America and extends westward to the central tropical Pacific Ocean. Both of the systems promote the aforementioned precipitation increase (Supplementary Material Figure S.3). Additionally, annual precipitation difference between the RLVS and the RLV only represents a tiny effect of soil feedback on precipitation, except for a decrease of 0.1–0.3 mm/day over South China southwestward to Thailand and Vietnam.

3.3. Data-model comparison

Using pollen, noble gas, plant macrofossils, speleothem, and lake status data, Farrera et al. (1999) compiled a set of mutually consistent paleoclimate estimates of mean annual surface temperature and mean surface temperature of the coldest month in the 32°N–33°S latitude band for the LGM. Combining these with botanical records from the former Soviet Union and Mongolia (Tarasov et al., 1999) and lake records from China (Yu et al., 2001), ten regions worldwide, i.e. western North America, northern South America, Central Africa, South Africa, equatorial eastern Africa, North Russia, India, middle-eastern China, South China, and North Australia, are chosen as examples to perform a data-model comparison here, at the same time taking the error of proxy estimates and the interannual variability, represented by standard deviation, of the simulated surface temperature in each of the four experiments into account.

It can be found from Table 1 that the IAP-AGCM alone (RL minus RC) produces well-known surface cooling at the LGM. The model, however, underestimates surface cooling magnitude reconstructed from a variety of proxy data over the above regions excluding North Russia. This is a general weakness of the PMIP fixed-SST AGCM simulations. It partly reflects the inadequacies of the reconstructed SST for the LGM (CLIMAP project members, 1981) because model-data disagreements over the tropics are generally less in the simulations derived from the PMIP computed-SST model (Pinot et al., 1999). On the whole,

Table 2
Climatic consequences due to vegetation feedback at the LGM in the previous simulations

Model and reference	LGM vegetation	Topography, ice sheet extent and thickness for the LGM	Vegetation-induced changes in surface temperature
GENESIS: atmosphere model (Crowley and Baum, 1997)	Reconstruction (Crowley, 1995)	ICE-4G (Peltier, 1994)	Annual cooling over eastern Eurasia, southwestern Europe, North Africa, and much of Australia, but warming over northern South America
BMRC: atmosphere model (Wyputta and McAvaney, 2001)	Reconstruction (Adams and Faure, 1997)	Topography and ice sheet extent (CLIMAP, 1981), ice sheet thickness (ICE-4G, Peltier, 1994)	Annual cooling over Eurasia, southern North America, high latitude North Atlantic, and Central Australia, but warming over northern North America
ECHAM3-BIOME1: asynchronously coupled atmosphere–biome model (Kubatzki and Claussen, 1998)	Simulated	Topography and ice sheet extent (CLIMAP, 1981), ice sheet thickness (ICE-3G, Tushingham and Peltier, 1991)	Cooling over middle and high latitude Eurasia and northeastern North America in winter and summer
GENESIS-IBIS: fully coupled atmosphere–vegetation model (Levis et al., 1999)	Simulated	ICE-4G (Peltier, 1994)	Annual cooling over mid-latitude Eurasian interior and western and central Australia, but warming over the rest of continents
HadSM3-TRIFFID: fully coupled atmosphere–vegetation–slab ocean model (Crucifix and Hewitt, 2005)	Simulated	ICE-4G (Peltier, 1994)	Annual cooling over middle and high latitude Eurasia and over the Arctic, but no changes over the rest of continents
CLIMBER-2: Earth system model of intermediate complexity (Jahn et al., 2005)	Simulated	ICE-4G (Peltier, 1994)	Annual cooling over middle and high latitude Eurasia and North Atlantic, but warming over southern high latitude

vegetation feedback (RLV minus RL) leads to significant surface cooling over these regions excluding western North America, especially over Central Africa, equatorial eastern Africa, India, middle-eastern China, South China, and North Australia. Moreover, vegetation-concomitant soil feedback (RLVS minus RLV) further induces additional surface cooling over India, North Russia, and North Australia. Therefore, vegetation and soil feedbacks simulated by the newly coupled IAP-AGCM/BIOME3 system partly reduce data-model discrepancies as indicated by the IAP-AGCM alone. As such, the above feedbacks should be taken into account if one aims to simulate the LGM climate realistically. Of course, the soil feedback put forward here needs to be further examined by similar experiments conducted by other climate system models.

4. Concluding remarks

An asynchronously coupled system between the IAP-AGCM and BIOME3 is set up in the present study. The IAP-AGCM/BIOME3 is then used to investigate the influences of vegetation and soil feedbacks on the LGM climate. It is found that the vegetation feedback alone can give rise to an annual surface cooling of 0.31 °C over the LGM ice-free continental areas.

When compared with previous studies either with reconstructed vegetation or a coupled model (Table 2), it is found that there are large uncertainties with respect to vegetation feedback at the LGM, particularly on a regional scale. For example, the simulated magnitude of global surface cooling due to vegetation feedback varies from 0.07 °C (IAP-AGCM/BIOME3), 0.3 °C (Wyputta and McAvaney, 2001), to 0.6 °C (Crucifix and Hewitt, 2005; Jahn et al., 2005). As far as coupled models are concerned, surface cooling over Eurasia produced by the IAP-AGCM/BIOME3 and CLIMBER-2 (Jahn et al., 2005) is weaker than those in the others, surface cooling over North Africa in the IAP-AGCM/BIOME3 is peculiar, and so on. Every model system is characterized by slightly or significantly different dynamical framework, physical processes, parameterization schemes, resolution, and so on. We therefore cannot expect identical results even if climate models are forced by the same forcings such as that within the protocol of the PMIP (Joussaume and Taylor, 1995). Additionally, topography and ice sheet extent and thickness data are different among the models, and atmospheric CO_2 concentration varies from 190 ppmv (CLIMBER-2) to 220 ppmv (GENESIS). All of these, together with experimental design, contribute in a complex manner to inter-model discrepancies. Given the highly nonlinear response of model system to forcing conditions, it is hence difficult to determine cause and effect in these simulations. Collectively, it can be drawn from Table 2 and the present study that vegetation feedback is an important process at the LGM, and it can induce additional surface cooling over much of Eurasia and Australia. In the future, more investigations are called for so as to constrain inter-model discrepancies and to obtain robust common climate responses due to vegetation feedback at the LGM.

It is further revealed here that vegetation-dominated soil feedback can add to vegetation-induced cooling over high latitude Eurasia and from the eastern Middle East eastward to the Indian Peninsula significantly. Compared to the IAP-AGCM alone, the vegetation and soil feedbacks can induce an additional global surface cooling of 0.13 °C (0.38 °C over the LGM ice-free continental areas), and the corresponding annual surface cooling reaches 0.74 °C, 0.54 °C, 0.34 °C, and 0.45 °C over the LGM ice-free continental areas within the 60°–90°N, 0°–30°N, 0°–30°S, and 30°N–30°S latitude bands, respectively. Therefore, the discrepancy between the IAP-AGCM alone and the proxy estimates can be partly reduced in some regions such as Central Africa, the Indian Peninsula, South China, and North Australia.

Finally, I would like to stress that the vegetation-dominated changes in soil characteristics assumed in the RLVS may be unrealistic. As an alternative approach for future climate modellers, interactive soil models where soil textures and colours interact with changes in vegetation and surface atmosphere in a more realistic manner should be implemented. In addition, it can be found from Table 2 that ocean dynamics is hitherto neglected when vegetation feedback at the LGM was examined. To what extent vegetation feedback influences the LGM climate in coupled atmosphere–ocean–vegetation models needs to be explored.

Acknowledgements

I would like to sincerely thank Prof. I. Colin Prentice for the assistance with BIOME3, two anonymous reviewers and Prof. Huijun Wang for the valuable comments on earlier drafts, and Dr. Julia Marshall and Editor for the English expression. Funding was jointly provided by the Chinese Academy of Sciences under Grant No. KZCX2-YW-205 and the National Science Foundation of China under Grant Nos. 40505017, 40405015, and 40775052.

Appendix A. Supplementary data

Supplementary data associated with this article can be found, in the online version, at doi:10.1016/j.palaeo.2008.07.023.

References

Adams, J.M., Faure, H., 1997. Preliminary vegetation maps of the world since the Last Glacial Maximum: an aid to archaeological understanding. J. archaeol. sci. 24, 623–647.
Barnola, J.M., Raynaud, D., Korotkevich, Y.S., Lorius, C., 1987. Vostok ice core provides 160,000-year record of atmospheric CO_2. Nature 329, 408–414.
Berger, A.L., 1978. Long-term variations of daily insolation and quaternary climatic changes. J. Atmos. Sci. 35, 2362–2367.
Bigelow, N.H., Brubaker, L.B., Edwards, M.E., Harrison, S.P., Prentice, I.C., Anderson, P.M., Andreev, A.A., Bartlein, P.J., Christensen, T.R., Cramer, W., Kaplan, J.O., Lozhkin, A.V., Matveyeva, N.V., Murray, D.F., McGuire, A.D., Razzhivin, V.Y., Ritchie, J.C., Smith, B., Walker, D.A., Gajewski, K., Wolf, V., Holmqvist, B.H., Igarashi, Y., Kremenetskii, K., Paus, A., Pisaric, M.F.J., Volkova, V.S., 2003. Climate change and Arctic ecosystems: 1. Vegetation changes north of 55°N between the Last Glacial Maximum, mid-Holocene, and present. J. Geophys. Res. 108 (D19), 8170. doi:10.1029/2002JD002558.
Braconnot, P., Otto-Bliesner, B., Harrison, S., Joussaume, S., Peterchmitt, J.-Y., Abe-Ouchi, A., Crucifix, M., Driesschaert, E., Fichefet, Th., Hewitt, C.D., Kageyama, M., Kitoh, A., Laîné, A., Loutre, M.-F., Marti, O., Merkel, U., Ramstein, G., Valdes, P., Weber, S.L., Yu, Y., Zhao, Y., 2007. Results of PMIP2 coupled simulations of the Mid-Holocene and Last Glacial Maximum — part 1: experiments and large-scale features. Clim. Past 3, 261–277.
Cane, M.A., Braconnot, P., Clement, A., Gildor, H., Joussaume, S., Kageyama, M., Khodri, M., Paillard, D., Tett, S., Zorita, E., 2006. Progress in paleoclimate modeling. J. Climate 19, 5031–5057.
Claussen, M., 1994. Coupling global biome models with climate models. Climate Res. 4, 203–221.
Claussen, M., 1997. Modeling bio-geophysical feedback in the African and Indian monsoon region. Clim. Dyn. 13, 247–257.
CLIMAP Project Members, 1981. Seasonal reconstructions of the Earth's surface at the Last Glacial Maximum. Geological Society of America Map Chart Series MC-36, Geol. Soc. Am., Boulder, Colorado.
Crowley, T.J., 1995. Ice age terrestrial carbon changes revisited. Glob. biogeochem. cycles 9, 377–389.
Crowley, T.J., Baum, S.K., 1997. Effect of vegetation on an ice-age climate model simulation. J. Geophys. Res. 102 (D14), 16463–16480.
Crucifix, M., Hewitt, C.D., 2005. Impact of vegetation changes on the dynamics of the atmosphere at the Last Glacial Maximum. Clim. Dyn. 25, 447–459.
Crucifix, M., Braconnot, P., Harrison, S.P., Otto-Bliesner, B., 2005. Second phase of Paleoclimate Modelling Intercomparison Project. Eos Trans. AGU 86 (28), 264.
Farrera, I., Harrison, S.P., Prentice, I.C., Ramstein, G., Guiot, J., Bartlein, P.J., Bonnefille, R., Bush, M., Cramer, W., von Grafenstein, U., Holmgren, K., Hooghiemstra, H., Hope, G., Jolly, D., Lauritzen, S.-E., Ono, Y., Pinot, S., Stute, M., Yu, G., 1999. Tropical climates at the Last Glacial Maximum: a new synthesis of terrestrial palaeoclimate data. I. Vegetation, lake-levels and geochemistry. Clim. Dyn. 15, 823–856.
Harrison, S.P., Prentice, I.C., 2003. Climate and CO_2 controls on global vegetation distribution at the Last Glacial Maximum: analysis based on palaeovegetation data, biome modelling and palaeoclimate simulations. Glob. chang. biol. 9, 983–1004.
Haxeltine, A., Prentice, I.C., 1996. BIOME3: An equilibrium terrestrial biosphere model based on ecophysiological constraints, resource availability, and competition among plant functional types. Glob. biogeochem. cycles 10, 693–709.
Jahn, A., Claussen, M., Ganopolski, A., Brovkin, V., 2005. Quantifying the effect of vegetation dynamics on the climate of the Last Glacial Maximum. Clim. Past 1, 1–7.
Jansen, E., Overpeck, J., Briffa, K.R., Duplessy, J.-C., Joos, F., Masson-Delmotte, V., Olago, D., Otto-Bliesner, B., Peltier, W.R., Rahmstorf, S., Ramesh, R., Raynaud, D., Rind, D.,

Solomina, O., Villalba, R., Zhang, D., 2007. Palaeoclimate. In: Solomon, S., Qin, D., Manning, M., Chen, Z., Marquis, M., Averyt, K.B., Tignor, M., Miller, H.L. (Eds.), Climate Change 2007: The Physical Science Basis. Contribution of Working Group I to the Fourth Assessment Report of the Intergovernmental Panel on Climate Change. Cambridge University Press, Cambridge, United Kingdom.

Jiang, D., Wang, H.-J., Drange, H., Lang, X., 2003. Last Glacial Maximum over China: sensitivities of climate to paleovegetation and Tibetan ice sheet. J. Geophys. Res. 108 (D3), 4102. doi:10.1029/2002JD002167.

Jiang, D., Wang, H.-J., Ding, Z., Lang, X., Drange, H., 2005. Modeling the middle Pliocene climate with a global atmospheric general circulation model. J. Geophys. Res. 110, D14107. doi:10.1029/2004JD005639.

Jin, L., Wang, H.-J., Chen, F., Jiang, D., 2006. A possible impact of cooling over the Tibetan Plateau on the mid-Holocene East Asian monsoon climate. Adv. Atmos. Sci. 23, 543–550.

Ju, L., Wang, H.-J., Jiang, D., 2007. Simulation of the Last Glacial Maximum climate over East Asia with a regional climate model nested in a general circulation model. Palaeogeogr. palaeoclimatol. palaeoecol. 248, 376–390.

Jolly, D., Haxeltine, A., 1997. Effect of low glacial atmospheric CO_2 on tropical African montane vegetation. Science 276, 786–788.

Joussaume, S., Taylor, K.E., 1995. In: Gates, W.L. (Ed.), Status of the Paleoclimate Modeling Intercomparison Project (PMIP), in Proceedings of the First International AMIP Scientific Conference. World Meteorol. Org., Geneva, pp. 425–430. WCRP-92, WMO/TD-732.

Kageyama, M., Laîné, A., Abe-Ouchi, A., Braconnot, P., Cortijo, E., Crucifix, M., de Vernal, A., Guiot, J., Hewitt, C.D., Kitoh, A., Kucera, M., Marti, O., Ohgaito, R., Otto-Bliesner, B., Peltier, W.R., Rosell-Melé, A., Vettoretti, G., Weber, S.L., Yu, Y., MARGO Project Members, 2006. Last Glacial Maximum temperatures over the North Atlantic, Europe and western Siberia: a comparison between PMIP models, MARGO sea-surface temperatures and pollen-based reconstructions. Quat. Sci. Rev. 25, 2082–2102.

Kaplan, J.O., Bigelow, N.H., Prentice, I.C., Harrison, S.P., Bartlein, P.J., Christensen, T.R., Cramer, W., Matveyeva, N.V., McGuire, A.D., Murray, D.F., Razzhivin, V.Y., Smith, B., Walker, D.A., Anderson, P.M., Andreev, A.A., Brubaker, L.B., Edwards, M.E., Lozhkin, A.V., 2003. Climate change and Arctic ecosystems: 2. Modeling, paleodata-model comparisons, and future projections. J. Geophys. Res. 108 (D19), 8171. doi:10.1029/2002JD002559.

Kubatzki, C., Claussen, M., 1998. Simulation of the global bio-geophysical interactions during the Last Glacial Maximum. Clim. Dyn. 14, 461–471.

Kutzbach, J., Bonan, G., Foley, J., Harrison, S.P., 1996. Vegetation and soil feedbacks on the response of the African monsoon to orbital forcing in the early to middle Holocene. Nature 384, 623–626.

Kutzbach, J., Gallimore, R., Harrison, S., Behling, P., Selin, R., Laarif, F., 1998. Climate and biome simulations for the past 21,000 years. Quat. sci. rev. 17, 473–506.

Leemans, R., Cramer, W., 1991. The IIASA Climate Database for Mean Monthly Values of Temperature, Precipitation and Cloudiness on a Terrestrial Grid. International Institute for Applied Systems Analysis, Laxenburg. RR-91-18.

Levis, S., Foley, J.A., Pollard, D., 1999. CO_2, climate, and vegetation feedbacks at the Last Glacial Maximum. J. Geophys. Res. 104 (D24), 31191–31198.

Levis, S., Bonan, G.B., Bonfils, C., 2004. Soil feedback drives the mid-Holocene North African monsoon northward in fully coupled CCSM2 simulations with a dynamic vegetation model. Clim. Dyn. 23, 791–802.

Liang, X.Z., 1996. Description of a nine-level grid point atmospheric general circulation model. Adv. Atmos. Sci. 13, 269–298.

Matthews, E., 1983. Global vegetation and land use: new high resolution data bases for climate studies. J. Clim. Appl. Meteorol. 22, 474–487.

Peltier, W.R., 1994. Ice age paleotopography. Science 265, 195–201.

Peltier, W.R., 2004. Global glacial isostasy and the surface of the ice-age earth: the ICE-5G (VM2) model and GRACE. Annu. rev. earth planet. sci. 32, 111–149.

Pinot, S., Ramstein, G., Harrison, S.P., Prentice, I.C., Guiot, J., Stute, M., Joussaume, S., 1999. Tropical paleoclimates at the Last Glacial Maximum: comparison of Paleoclimate Modeling Intercomparison Project (PMIP) simulations and paleodata. Clim. Dyn. 15, 857–874.

PMIP, 2000. Paleoclimate Modeling Intercomparison Project (PMIP). Proceedings of the Third PMIP Workshop, WCRP-111, WMO/TD-No. 1007, p. 271.

Prentice, I.C., Jolly, D., BIOME 6000 participants, 2000. Mid-Holocene and glacial-maximum vegetation geography of the northern continents and Africa. J. biogeogr. 27, 507–519.

Prentice, I.C., Harrison, S.P., Jolly, D., Guiot, J., 1998. The climate and biomes of Europe at 6000 yr BP: comparison of model simulations and pollen-based reconstruction. Quat. sci. rev. 17, 659–668.

Ramstein, G., Kageyama, M., Guiot, J., Wu, H., Hély, C., Krinner, G., Brewer, S., 2007. How cold was Europe at the Last Glacial Maximum? A synthesis of the progress achieved since the first PMIP model-data comparison. Clim. Past 3, 331–339.

Tarasov, P.E., Peyron, O., Guiot, J., Brewer, S., Volkova, V.S., Bezusko, L.G., Dorofeyuk, N.I., Kvavadze, E.V., Osipova, I.M., Panova, N.K., 1999. Last Glacial Maximum climate of the former Soviet Union and Mongolia reconstructed from pollen and plant macrofossil data. Clim. Dyn. 15, 227–240.

Texier, D., de Noblet, N., Harrison, S.P., Haxeltine, A., Jolly, D., Joussaume, S., Laarif, F., Prentice, I.C., Tarasov, P., 1997. Quantifying the role of biosphere–atmosphere feedbacks in climate change: coupled model simulations for 6000 years BP and comparison with palaeodata for northern Eurasia and northern Africa. Clim. Dyn. 13, 865–882.

Tushingham, A.M., Peltier, W.R., 1991. Ice-3G: a new global model of Late Pleistocene deglaciation based upon geophysical predictions of post-glacial relative sea level change. J. Geophys. Res. 96 (B3), 4497–4523.

Wang, H.-J., 2002. The mid-Holocene climate simulated by a grid-point AGCM coupled with a biome model. Adv. Atmos. Sci. 19, 205–218.

Wei, J., Wang, H.-J., 2004. A possible role of solar radiation and ocean in the mid-Holocene East Asian monsoon climate. Adv. Atmos. Sci. 21, 1–12.

Wilson, M.F., Henderson-Sellers, A., 1985. A global archive of land cover and soils data for use in general circulation climate models. J. Climatol. 5, 119–143.

Wyputta, U., McAvaney, B.J., 2001. Influence of vegetation changes during the Last Glacial Maximum using the BMRC atmospheric general circulation model. Clim. Dyn. 17, 923–932.

Yu, G., Xue, B., Liu, J., Chen, X., Zheng, Y.Q., 2001. Lake Records from China and the Palaeoclimate Dynamics. China Meteorological Press, Beijing, pp. 102–104.

Zhang, Z., Wang, H.-J., Guo, Z., Jiang, D., 2007a. Impacts of tectonic changes on the reorganization of the Cenozoic paleoclimatic patterns in China. Earth planet. sci. lett. 257, 622–634.

Zhang, Z., Wang, H.-J., Guo, Z., Jiang, D., 2007b. What triggers the transition of palaeoenvironmental patterns in China, the Tibetan Plateau uplift or the Paratethys Sea retreat? Palaeogeogr. palaeoclimatol. palaeoecol. 245, 317–331.